ELSEVIER

Biochimica et Biophysica Acta 1282 (1996) 48–56

BBA Biochimica et Biophysica Acta

A kinetic characterization of putrescine and spermidine uptake and export in human erythrocytes

Gary H. Fukumoto [a], Craig V. Byus [b,*,1]

[a] *Department of Biochemistry, University of California, Riverside, Riverside, CA 92521-0121, USA*
[b] *Division of Biomedical Sciences, University of California, Riverside, Riverside, CA 92521-0121, USA*

Received 29 March 1995; accepted 24 January 1996

Abstract

Using human erythrocytes as a model system for the study of mammalian polyamine transport, detailed kinetic parameters regarding the uptake and export of putrescine and spermidine were determined. The putrescine uptake data indicated a multi-component uptake system comprised of a low-capacity saturable component and a non-saturable component. The saturable putrescine uptake component demonstrated a calculated K_m of 21.0 μM and a V_{max} of only 6.52×10^{-13} M/s. The non-saturable linear putrescine uptake rate was defined by a significant pH dependence, a lack of uptake inhibition by related polyamines, and a permeability π of 3.19×10^{-8} s^{-1}. These findings suggested that non-saturable putrescine uptake involved a process of simple diffusion. Spermidine uptake exhibited Michaelis-Menten kinetics with a K_m and V_{max} of 12.5 μM and 1.36×10^{-12} M/s, respectively. Spermidine uptake did not demonstrate pH dependence and was not significantly inhibited by any of the tested polyamines. The Arrhenius plot of spermidine uptake was determined to be biphasic with calculated activation energies of spermidine uptake of 135.2 kJ/mol for 19–21°C and 59.3 kJ/mol for 21–35°C. These data suggest the possibility of multiple spermidine uptake processes which are not mediated by simple diffusion across the cell membrane. The putrescine export process demonstrated both saturable and non-saturable components. The calculated K_m, V_{max} and π for putrescine export were 33.8 μM, 1.19×10^{-11} M/s and 2.81×10^{-7} s^{-1}, respectively. The spermidine export process was non-saturable up to intracellular spermidine concentrations of 4 μM. At similar intracellular and extracellular concentrations of putrescine and spermidine, however, export processes displayed rates which were an order of magnitude greater than their respective uptake rates. This finding supports the possible presence of mediated putrescine and spermidine export processes different than simple diffusion.

Keywords: Putrescine; Spermidine; Transport; Erythrocyte; Uptake; Export

1. Introduction

A wide variety of polyamine uptake processes have been described for many different mammalian cell systems [1–8]. Both specific and non-specific transporters of putrescine and spermidine have been reported with varying rates, affinities and substrate dependences [1–11]. Along with polyamine biosynthesis and turnover, these polyamine uptake processes have been implicated in the regulation and maintenance of intracellular polyamine concentrations in mammalian cells undergoing growth and differentiation [12–23].

Less is known, however, about polyamine export from mammalian cells. While the molecular basis of putrescine export has been extensively characterized in prokaryotes [24], much less is known about this process in mammalian systems [25–35]. This lab has recently reported that the constitutive export of putrescine and cadaverine occurred in a variety of cultured cells under serum-free conditions [26]. Furthermore, this putrescine export process appeared to be highly regulated by hormones, growth factors and serum with selective inhibition by diamines and verapamil [36]. Thus, in conjunction with polyamine turnover, this export process could serve to lower intracellular polyamine concentrations in response to various effectors and cellular metabolism.

In order to thoroughly characterize the uptake and export processes in mammalian cells, accurate quantitative measurements of intracellular polyamine concentrations and net transport rates were required. Since most cultured

* Corresponding author. Fax: +1 (909) 7873590; e-mail: byus@citrus.ucr.edu.

[1] Supported by NIH ES06128 and DOE contract DEA1AO-85 CD 76260.

PII S0005-2736(96)00036-3

mammalian cells have non-uniform cell volumes and contain interchangeable intracellular polyamine pools, they were not considered good models for rigorous kinetic characterization.

Even though they have low endogenous polyamine levels, human erythrocytes were considered an appropriate model system in which to study polyamine uptake and export for several reasons. Uniform cell dimensions, water volumes and membrane compositions are explicitly and accurately known for erythrocytes from different species [36]. These data make calculations of transport rates from erythrocytes much more accurate than from cultured cells or membrane vesicles.

In addition, hematopoietic stem cells contain a large number of membrane transporters similar to other mammalian cell types. During hematopoiesis, however, a number of transporters are reduced 100-fold or more [37–39]. Along with the expulsion of the nucleus, this overall reduction of membrane proteins produces a much simplified cell with little intracellular compartmentalization. Erythrocytes, therefore, represent a natural vesicle model of the stem cells which can be used to characterize transport rates.

By incubating these cells with varying extracellular concentrations of putrescine or spermidine, kinetic parameters were obtained which described the uptake and efflux transport rates and their saturabilities. In contrast to earlier preliminary polyamine transport studies in erythrocytes [9,40], all assays were performed under serum-free conditions. Since high levels of polyamines have been found to be reversibly bound in serum, using serum-free conditions allowed for a more accurate quantification of true polyamine concentrations, transport rates and saturation kinetics. Competitive effects on uptake by additional polyamines were also measured. It was determined that at equivalent intracellular and extracellular concentrations of putrescine and spermidine, efflux occurred approximately ten times faster than uptake for both tested polyamines.

2. Materials and methods

2.1. Materials

[^{3}H]Putrescine was obtained from Amersham Life Science while [^{3}H]spermidine was purchased from NEN Research Products. RPMI 1640 was purchased from Gibco-BRL. Cytoscint liquid scintillation cocktail was purchased from ICN Biochemicals. All other reagents were obtained from Sigma.

2.2. Erythrocyte preparation

Erythrocytes were prepared as described [9] with slight modifications. Briefly, blood was drawn and mixed with 10% v/v 0.1 M sodium citrate as an anti-coagulant. Cells were immediately centrifuged at $2000 \times g$ for 15 min. Serum was collected and the white buffy coat discarded. Cells were resuspended and centrifuged twice in 0.22 μm filtered sterile RPMI 1640 media, pH 7.4 with 20 mM Hepes. Cells were then placed at 50% hematocrit and pipetted into 100 μl aliquots in autoclaved 1.5 ml microfuge tubes. Erythrocytes were stored at 4°C for no more than 3 days.

Cell number was initially determined for preparations by two methods: cell dry weight and a Neubauer cell counting chamber. Aliquots of erythrocytes were dried overnight at 70°C until no weight changes were observed. Hematological dry cell weight was obtained from reference works [36,42] and was taken to be 3.0×10^{-11} g/cell. Neubauer cell counts used Hayem red cell counting solution for cell dilution and were performed twice. Both methods gave nearly identical values such that the cell dry weight method alone was eventually used.

2.3. Determination of extracellular and intracellular polyamine levels in serum-free human erythrocytes by HPLC

Erythrocytes were incubated in RPMI, pH 7.4 at 37°C. After specified intervals, samples were centrifuged and analyzed as per Gilbert et al. [41]. Briefly, collected media was run through Bio-Rex 70 ion-exchange resin, washed and eluted with 4.0 M NH_4OH. Eluants were vacuum centrifuged to dryness, dansylated and submitted to HPLC analysis. Washed cells were lysed in 0.5 M perchloric acid (PCA) by sonication. Samples were centrifuged, dansylated and analyzed by HPLC.

Though the levels were quite low in comparison to mammalian cell lines, putrescine and spermidine concentrations in erythrocytes were reproducibly measured. Due to the high degree of clean-up provided by the analytical HPLC method [41] and the use of serum-free conditions, background polyamine levels were reduced to allow a greater sensitivity of detection and quantitation compared to previous studies. A large cell number per assay (approx. 10^8 cells/assay) also improved the detection of the low intracellular polyamine levels present in untreated erythrocytes. Typical estimates from our laboratory of intracellular putrescine concentrations in mammalian cell lines range from 1 to 10 μM while erythrocytes demonstrated intracellular concentrations in the nM range. A value of 90 fl for the erythrocyte cell volume [42] was used to calculate the intracellular polyamine concentrations.

Human sera from the erythrocyte preparations were also analyzed for polyamine content by HPLC. Briefly, a 500 μl aliquot of human serum was placed in 0.5 M PCA for protein precipitation. Samples were centrifuged and the supernatant was saved. A 500 μl aliquot of this supernatant was dansylated and analyzed by HPLC as described [41].

2.4. Erythrocyte net uptake assays

Aliquoted erythrocytes were equilibrated at 37°C for 5 min before assays. Radiolabelled polyamines were added at $t = 0$. Following the indicated time periods, aliquots were washed three times with ice-cold phosphate-buffered saline (PBS). Erythrocyte pellets were lysed with 0.5 M perchloric acid, sonicated and stored overnight at −20°C. The samples were centrifuged at $12000 \times g$ for 7 min. Aliquots of the supernatant were then counted. Possible quenching from hemoglobin was not detected as determined from the H number.

For the pH-dependent uptake assays, RPMI, 20 mM Hepes was adjusted to the desired pH using dilute HCl or NaOH solutions and then sterile filtered with a 0.22 μm filter. Uptake was performed as previously described.

2.5. Erythrocyte net efflux assays

Erythrocytes were incubated at 37°C in radiolabelled spermidine or putrescine of different concentrations for 15, 30 or 60 min. After this loading period, the cells were washed rapidly with ice-cold PBS and reincubated in fresh RPMI at 37°C over the indicated efflux time periods. These cells were rewashed and assayed for efflux as above. The measured decrease of radiolabel in the cells with time was taken to represent the amount of effluxed polyamine.

2.6. Calculated concentration-dependent uptake and export of putrescine and spermidine using determined kinetic constants from transport assays

Saturation curves detailing the saturable components of putrescine export and uptake were plotted using the kinetic constants determined from uptake and export assays and the Michaelis-Menten equation for saturable kinetics, $v = (V_{max} * S)/(K_m + S)$, where v is the transport velocity (M/s), V_{max} is the maximum transport velocity (M/s), K_m is the Michaelis constant (M) and S is the concentration of *cis*-applied putrescine (M). The total uptake and export curves were determined by plotting both saturable and non-saturable components of putrescine uptake and export using the modified Michaelis-Menten equation, $v = (V_{max} * S)/(K_m + S) + (\pi * S)$, where π is the rate constant of the non-saturable transport process (s^{-1}).

The saturable spermidine uptake curve was plotted as described for the saturable putrescine process. The non-saturable spermidine export curve was determined by plotting $v = \pi * S$, where v is the spermidine export rate, π is the non-saturable rate constant of spermidine export and S is the intracellular concentration of spermidine.

3. Results

3.1. Determination of intracellular and extracellular polyamine concentrations in human erythrocytes assayed under serum-free conditions

The observed basal concentration of intracellular putrescine was determined as approximately 1 nM and did not change significantly over the incubation period (Fig. 1A). Net export of putrescine into the culture media was observed only during the initial 15 min of incubation with media putrescine levels remaining constant over the ensuing 45 min. Intracellular spermidine levels increased slightly over the initial 30 min incubation period (Fig. 1B). The basal intracellular spermidine concentration was also quite low i.e. 7 nM. Compared to putrescine export, spermidine export did not occur to an appreciable extent and was not within the limit of quantitation of the analytical HPLC method [41]. The low intracellular polyamine levels were in agreement with the observation that the export rate was ten-fold faster than the uptake rate. The observed increase in total putrescine was also consistent with the reported limited degree of polyamine biosynthesis [43].

Human serum obtained during the preparation of the erythrocytes had typical putrescine concentrations of 100–300 nM while spermidine and spermine levels were less than 1 nM. N^1-acetylputrescine was also detected extracellularly with concentrations less than 100 nM.

3.2. Concentration-dependent uptake of putrescine by human erythrocytes

In order to determine the initial linear region of the proposed time-dependent uptake process, putrescine uptake was assayed over a 60 min interval with an extracellular concentration of 100 μM (data not shown). High linearity

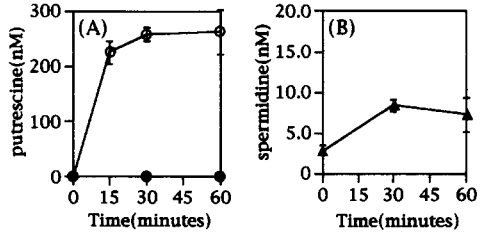

Fig. 1. Time-dependent changes in the intracellular and extracellular putrescine and spermidine levels in isolated human erythrocytes. Red blood cells were incubated at 37°C in RPMI, pH 7.4 containing 20 mM Hepes. The intracellular and extracellular levels of putrescine (A) and spermidine (B) over a 60 min period were determined as described in Materials and methods. Data is represented as the mean ± SEM for three determinations. ● = intracellular putrescine, ○ = extracellular putrescine, ▲ = intracellular spermidine. Trace levels of extracellular spermidine were also detected below the limit of quantification, i.e. femtomolar or 10^{-15} M range.

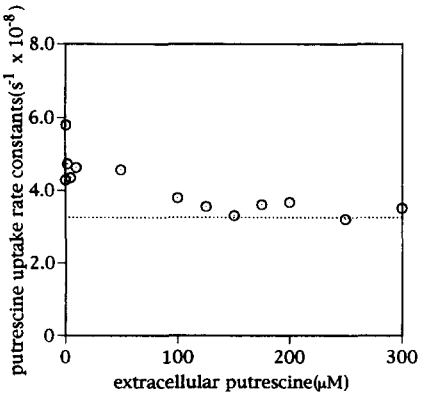

Fig. 2. Concentration dependence of the putrescine uptake rate constant k. The rate constant k of the putrescine uptake process in human erythrocytes was plotted over a range of extracellular putrescine concentrations. The dashed line represents the permeability π which k approaches at increasing extracellular putrescine concentrations. The permeability π was determined to be 3.19×10^{-8} s^{-1}.

was observed over the first 15 min of uptake. Subsequent measurements were determined in triplicate at 1, 2, 3 and 5 min for the indicated putrescine concentrations. Analysis of the putrescine uptake rate constants over a range of extracellular putrescine concentrations demonstrated an initial decrease with a convergence to a non-zero asymptote (Fig. 2) indicating the presence of saturable and non-saturable uptake components. The putrescine uptake data was curve-fit to the Michaelis-Menten equation with a linear non-saturable component using the Levinson-Marquardt iterative method of approximation (Fig. 3). The calculated values of K_m, V_{max}, and permeability π were 21.0 μM, 6.52×10^{-13} M/s, and 3.19×10^{-8} s^{-1}, respectively. The goodness of fit for this curve fit was 0.995.

Due to the large contribution of the linear non-saturable component to the overall putrescine uptake process, additional statistical analyses were performed to assess the curve-fit model. An inspection of the residuals, defined as the difference of observed data from the calculated curve fit, was done for both the proposed model and a simple linear curve fit. A linear curve fit increasingly overestimated the observed putrescine uptake rate as the extracellular putrescine concentration decreased below 10 μM (data not shown). Conversely, a Michaelis-Menten curve fit demonstrated small residuals below 10 μM with increasing random differences with increasing extracellular putrescine concentrations.

3.3. Determination of the pH dependence and the activation energy E_a for putrescine uptake

The putrescine uptake rate measured at an extracellular putrescine concentration of 100 μM exhibited a two-fold decrease with a two unit decrease of pH (data not shown). By using the Henderson-Hasselbach equation and graphing the rate versus the derived concentrations of uncharged putrescine, a linear dependence could be seen.

To define the temperature dependence of putrescine uptake, uptake assays were conducted from 19–35°C over 2 min. The rate constants were determined by assuming first-order reaction kinetics [44,45]. Using the Arrhenius equation to plot, ln k vs. $1/T$, the slope '$-E_a/R$' was found to be biphasic with a breakpoint at 21°C (Fig. 4). The energies of activation E_a of putrescine uptake were thus determined to be 86.1 kJ/mol from 19 to 21°C and 18.8 kJ/mol from 21 to 35°C.

Assays of putrescine uptake in the presence of other polyamines indicated a slight increase in uptake rate with addition of extracellular cadaverine, spermidine, and sper-

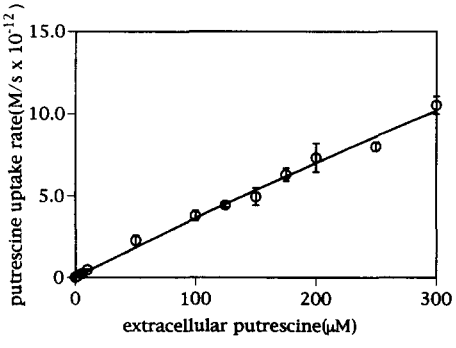

Fig. 3. Concentration-dependent putrescine uptake in human erythrocytes. Putrescine uptake in erythrocytes contained both saturable and non-saturable components. Using the Levinson-Marquardt iterative method, the data was curve-fit to the equation, $v=(V_{max}*S)/(K_m+S)+(\pi*S)$, where v is the reaction velocity, S is the extracellular putrescine concentration and $\pi*S$ represents the non-saturable component of uptake. The calculated values of V_{max}, K_m and π are 6.52×10^{-13} M/s, 21.0 μM, 3.19×10^{-8} s^{-1}, respectively. The goodness-of-fit for this calculated curve was 0.995. Data is represented as the mean ± SEM for three determinations.

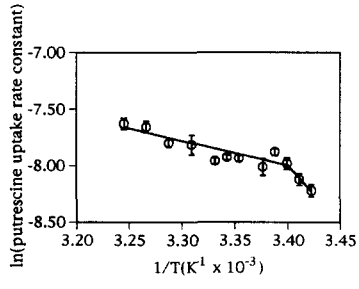

Fig. 4. Arrhenius plot of putrescine uptake. Assays were performed from 19 to 35°C with 0.4 μM extracellular putrescine. The temperature dependence of the putrescine uptake rate implied use of the Arrhenius equation, $\ln k = E_a/RT + \ln A$, where k = the rate constant, E_a = the activation energy, R = the gas constant, T = temperature, and A = the frequency factor. Data was plotted as ln k versus $1/T$ with the slope = $-E_a/R$. It was assumed that putrescine transport followed a unimolecular mechanism (i.e. no cation, anion or substrate co-dependence). The derived activation energies E_a were 86.1 kJ/mol from 19 to 21°C and 18.8 kJ/mol for 21–35°C. Data is represented as the mean ± SEM for three determinations.

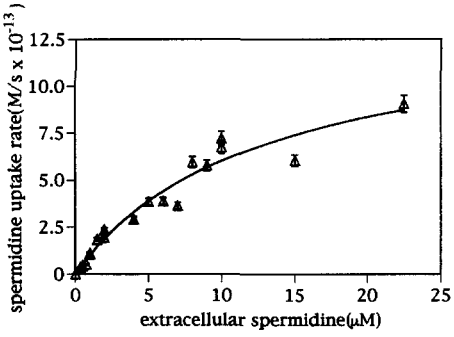

Fig. 5. Concentration dependence of spermidine uptake. Initial linear uptake rates of time-dependent spermidine uptake curves at the indicated concentrations were used to plot the concentration-dependent uptake of spermidine. The data was fit to the Michaelis-Menten equation using the Levinson-Marquardt iterative method. Regression analysis produced a goodness-of-fit coefficient of $R^2 = 0.95$. The calculated V_{max} and K_m for this curve fit were 1.36×10^{-12} M/s and 12.5 μM, respectively. Data is represented as the mean ± SEM for three determinations.

mine (data not shown). The concentration of each of the polyamines in the uptake assay was 100 μM.

3.4. Concentration-dependent uptake of spermidine by human erythrocytes

The spermidine uptake rate demonstrated saturable uptake kinetics over an observed concentration range of 0.33–10 μM spermidine (Fig. 5). The data was subsequently fit to the Michaelis-Menten equation to obtain kinetic parameters. The derived K_m and V_{max} were determined to be 12.5 μM and 1.36×10^{-12} M/s, respectively.

Exogenously applied polyamines at 10 times the extracellular spermidine levels did not show a significant effect on the rate of spermidine uptake in erythrocytes (data not shown). A small inhibitory effect may be attributed to putrescine but this inhibition was not statistically significant.

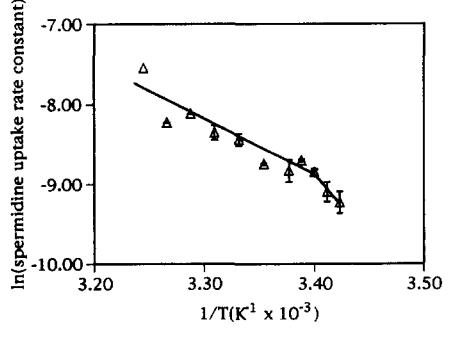

Fig. 6. Arrhenius plot of spermidine uptake. Spermidine uptake assays were performed at each temperature with 0.33 μM extracellular spermidine. The temperature dependence of the spermidine uptake rate implied the use of the Arrhenius equation, $\ln k = E_a/RT + \ln A$, where k = the rate constant, E_a = the activation energy, R = the gas constant, T = temperature, and A = the frequency factor. Data was plotted as $\ln k$ versus $1/T$ with the slope = $-E_a/R$. It was assumed that spermidine transport followed a unimolecular mechanism (i.e. no cation, anion or substrate dependence). The derived activation energies for 19–21°C and 19–35°C were 135.2 kJ/mol and 59.3 kJ/mol, respectively. Data is represented as the mean ± SEM for three determinations.

3.5. Determination of pH dependence and the activation energy E_a for spermidine uptake

As the pH was raised from 6 to 8, little alteration of the rate of spermidine uptake was observed (data not shown). Differences in the calculated uncharged spermidine concentrations also did not correlate significantly to the uptake rate though a strong dependence on temperature was seen (Fig. 6). Since the substrate co-dependence was unknown at this time, first-order reaction kinetics served as a first approximation. Using the Arrhenius equation, the resultant curve showed a breakpoint at 21°C. The activation energies of spermidine uptake were 135.2 kJ/mol for 19–21°C and 59.3 kJ/mol for 21–35°C.

3.6. Concentration dependence of putrescine and spermidine efflux

Only relatively low intracellular concentrations of putrescine and especially spermidine were obtainable since long-term loading and incubation of erythrocytes was avoided to minimize experimental error attributable to the potential metabolism and interconversion of intracellular putrescine and spermidine. Over an efflux time course of several minutes, the amounts of the labelled polyamines retained by the erythrocytes decreased linearly (data not shown). This measured initial putrescine efflux rate demonstrated both saturable and non-saturable components (Figs. 7 and 8). The K_m and V_{max} of putrescine efflux were determined to be 33.8 μM and 1.19×10^{-11} M/s.

The spermidine efflux rate displayed a linear non-saturable concentration dependence up to 3.5 μM (Fig. 9).

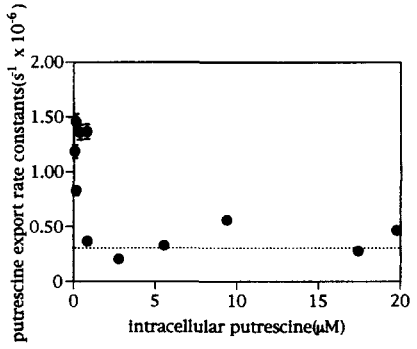

Fig. 7. Concentration dependence of the putrescine efflux rate constant k. The putrescine efflux rate constants were plotted over a range of intracellular putrescine concentrations. The dashed line represents the estimated permeability π which k approaches with increasing putrescine concentrations. The permeability π was determined to be 2.81×10^{-7} s^{-1}. Data is represented as the mean ± SEM for three determinations.

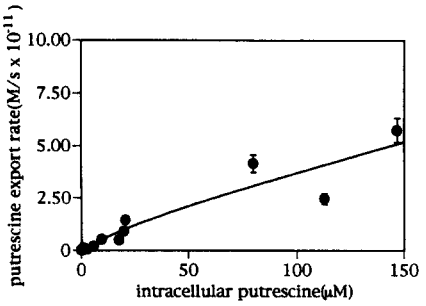

Fig. 8. Concentration-dependent putrescine efflux from human erythrocytes. Putrescine efflux from erythrocytes contained both saturable and non-saturable components. Using the Levinson-Marquardt iterative method, the data was curve-fit to the equation, $v = (V_{max} * S)/(K_m + S) + (\pi * S)$, where π represents the non-saturable component of efflux. The calculated values of V_{max}, K_m and π are 1.19×10^{-11} M/s, 33.8 μM and 2.81×10^{-7} s^{-1}. The goodness of fit for this calculated curve was 0.89. Data is represented as the mean ± SEM for three determinations.

The derived intracellular concentration-dependent rate constant from a linear plot of the data was 3.29×10^{-6} s^{-1}.

3.7. Comparison of the calculated concentration-dependent curves of putrescine and spermidine uptake and export using kinetic constants determined from transport assays

In order to compare the relative rates of putrescine transport into and out of the erythrocyte at a given putrescine level, the saturable and non-saturable components of putrescine export and uptake were plotted over a range of *cis*-applied concentrations (Fig. 10A). A consideration of both saturable and non-saturable components of putrescine export and uptake showed that the overall export process was an order of magnitude greater than the overall putrescine uptake process.

The saturable spermidine uptake process and the non-saturable spermidine export process were plotted up to

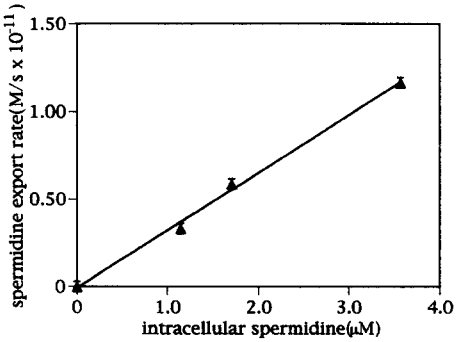

Fig. 9. Concentration dependence of spermidine efflux. Intracellular spermidine concentrations were determined by red cell volume and the amounts of spermidine uptaken. Spermidine efflux demonstrated a linear concentration dependence of 3.29×10^{-6} s^{-1} with increasing intracellular spermidine levels. Data is represented as the mean ± SEM for three determinations.

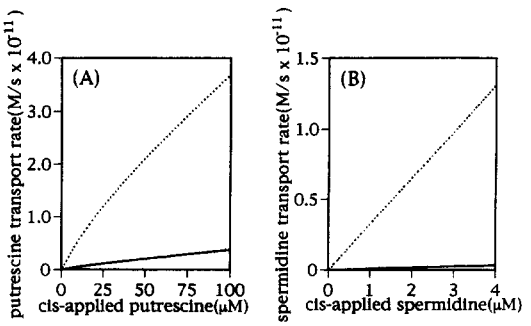

Fig. 10. Calculated concentration-dependent uptake and export for putrescine and spermidine using kinetic constants determined from transport assays. A: the putrescine uptake and export processes, comprised of saturable and non-saturable components, were plotted by using the determined K_m, V_{max} and permeability π from transport assays over the indicated concentration range. B: saturable spermidine uptake and non-saturable spermidine export were compared by using the determined K_m, V_{max} and permeability π from transport assays over the indicated concentration range. · · · = the export process, ——— = the uptake process.

cis-applied spermidine concentrations of 4 μM (Fig. 10B). Over this concentration range, non-saturable spermidine export was more than an order of magnitude greater than saturable spermidine uptake.

4. Discussion

The initial characterizations of the putrescine uptake system in erythrocytes showed a strong dependence of uptake rate on the extracellular putrescine concentration (Fig. 3). This concentration dependence of the putrescine uptake rate suggested a non-saturable mechanism involving simple diffusion of putrescine across the erythrocyte membrane (see below). However, the uptake rate constants at low extracellular putrescine concentrations demonstrated values which decreased asymptotically with increasing extracellular putrescine concentrations (Fig. 2). This decrease precluded a single component simple diffusion-mediated uptake process and indicated a putrescine uptake system with both saturable and non-saturable components. Some precedence for similar putrescine uptake processes has been reported in rat brush-border membrane vesicles [3,46] and porcine aortic endothelial cells [47].

Due to the large contribution of the linear non-saturable component to the overall putrescine uptake process, however, a linear curve fit to the data could not be immediately disregarded. A more sophisticated statistical analysis employing a measure of the residuals of a linear curve fit demonstrated an increasing systematic deviation of the observed putrescine uptake rate from the calculated linear curve with decreasing extracellular putrescine concentrations (data not shown). These large residuals would be expected over the log phase region of a saturable process and suggested that a linear curve fit was inappropriate. In

comparison, a residuals analysis of a Michaelis-Menten curve fit with a linear non-saturable component demonstrated small residual values at low extracellular putrescine concentrations and increasing random deviations with increasing concentrations. The observed random deviations at higher putrescine concentrations were attributable to the decreased sensitivity of the assay with lower specific activity. The overall assessment of the Michaelis-Menten curve fit thus appeared appropriate.

The calculated V_{max} of the saturable component in the putrescine uptake system of erythrocytes, 6.52×10^{-13} M/s, was similar to the V_{max} for the uptake system in human platelets [48] (i.e. 8.52×10^{-13} M/s; V_{max} value converted from original units using reference data as per Materials and methods). Since erythrocytes and platelets are both derived from hematopoietic stem cells, this similarity in putrescine uptake rate seems reasonable. In comparison, the calculated K_m of putrescine uptake in human erythrocytes was several times higher than comparative putrescine uptake systems in rat and rabbit brush-border membrane vesicles [3,46], human pulmonary artery endothelial cells [6], and B16 melanoma cells [1]. This higher K_m may have resulted from our use of serum-free conditions in the erythrocyte uptake assays. As noted previously, our lab has found variable levels of putrescine and spermidine in fetal bovine serum (i.e. up to 500 μM putrescine). With additional polyamine contributions from reversible binding to serum proteins [49], these serum polyamine levels may interfere with the accurate and quantitative determination of kinetic parameters.

In addition to a strong linear concentration dependence, the putrescine uptake rate showed a dependence on temperature. Such a temperature dependence is often characteristic of simple diffusion processes [50]. With an observed E_a of 18.8 kJ/mol from 21 to 35°C (Fig. 4), putrescine uptake compared favorably to the diffusion of low molecular weight alcohols across red cell membranes (i.e. 32 kJ/mol [50]). Since low temperatures induce a greater membrane rigidity and inhibit the function of membrane transport proteins, the higher E_a from 19 to 21°C did not represent an active transport mechanism and a simple diffusion process was implicated.

Further, no competitive inhibition by the other polyamines on the putrescine uptake rate was observed (data not shown). Such a result would be expected for a non-specific transport process such as simple diffusion across the cell membrane.

At physiological pH, however, putrescine exists largely as a divalent cation exhibiting a low permeability to the erythrocyte cell membrane. The hydrophobic interior of the lipid bilayer provides an effective barrier to electrolytes and greatly reduces ion transport by simple diffusion [51]. If simple diffusion were involved in the putrescine uptake process, the uncharged form of putrescine would be implicated as the nominal transported species due to its greater hydrophobicity. To test this possibility, the extracellular pH of the reaction mixture was raised to produce a greater proportion of uncharged extracellular putrescine. A distinct increase in putrescine uptake was demonstrated with increased pH. Since H^+ equilibrates rapidly between intracellular and extracellular spaces [52], differences of putrescine uptake rate with increasing pH were not attributable to a proton gradient. This observed acceleration of the putrescine uptake rate with increasing pH supported the possibility that simple diffusion was involved in the uptake process.

This two-fold increase in the putrescine uptake rate did not correlate proportionally with the calculated 100-fold increase in the uncharged putrescine concentration (data not shown). This result suggested that putrescine export, which exceeds putrescine uptake by an order of magnitude with similar *cis*-applied putrescine concentrations (Fig. 10A), was involved. Though putrescine uptake may have increased proportionally with pH increases of the reaction mixture, the overall uptake rate may have been moderated by a concomitant increase of the putrescine export rate.

Saturable kinetics for the uptake of spermidine were also observed in human erythrocytes (Fig. 5). Using a Michaelis-Menten curve fit on the direct plot of uptake rates versus concentrations, the K_m and V_{max} of spermidine uptake were determined to be 12.5 μM and 1.36×10^{-12} M/s. These values compare with the facilitated diffusion systems of arginine and lysine in human erythrocytes [50]. Since arginine and lysine are precursors to putrescine and cadaverine, respectively, some overall control of polyamine biosynthesis and intracellular level may be indicated.

Compared to spermidine uptake in other cell systems [1,3], however, saturable spermidine uptake in human erythrocytes occurred at a much lower rate. This result may have been due partially to the significant reduction of some membrane transporters that erythrocytes undergo in hematopoiesis. This high degree of differentiation and enucleation may significantly reduce the number of putative membrane transporters and thus the overall uptake rate. Although some investigators [1,4,40,53] report K_m values for spermidine uptake that are lower than was determined here, it should again be noted that many of those assays were performed in the presence of serum.

In contrast to putrescine uptake, spermidine uptake showed little dependence on pH changes (data not shown). No significant pH-dependent effect upon the spermidine uptake rate was seen by increasing the relative amounts of uncharged spermidine. This pH independence suggested that simple diffusion was not a prominent determinant of the spermidine uptake process. Rather, other mediated processes such as co-transport may be indicated.

Further evidence that spermidine uptake differs from putrescine uptake was demonstrated by the large effect of temperature on rate. The derived activation energies for 19–21°C and 21–35°C (E_{a1} and E_{a2}, respectively) showed a difference of approximately 80 kJ/mol (Fig. 6). This

large increase in activation energy indicated a severe inhibition or down-regulation of the spermidine uptake process with decreased temperature. Further, both E_a values greatly exceeded the E_a for putrescine uptake from 21 to 35°C, i.e., 18.8 kJ/mol (Fig. 4). Thus, significant spermidine uptake by simple diffusion appeared unlikely.

Extracellularly applied polyamines did not appear to affect the spermidine uptake rate to a large extent (data not shown). Though other investigators have reported both competitive and non-competitive inhibition of spermidine uptake by putrescine [1,3], the observed inhibition by putrescine on spermidine uptake in human erythrocytes was not statistically significant.

Though spermidine export did not demonstrate saturable kinetics up to 4 μM intracellular spermidine (Fig. 9), this non-saturable spermidine export rate was much greater than the saturable spermidine uptake rate with similar *cis*-applied spermidine concentrations (Fig. 10B). This difference in transport rates suggested the presence of a relatively high-capacity spermidine export process which could not be saturated under the specified assay conditions. The low intracellular spermidine level detected in vivo (i.e. approximately 7 nM) appeared to be in keeping with this greater export capacity. Due to the high comparative level of spermidine export, however, some process or series of processes must be present in human erythrocytes to prevent spermidine depletion. Some degree of coordinated polyamine biosynthesis may thus exist to maintain the intracellular spermidine levels depleted by the processes of spermidine degradation and export. In addition, reversible spermidine binding to cytoskeletal proteins and cell membranes may serve to maintain an intracellular pool of spermidine [11]. Along with a possible coordinated regulation of export and uptake rates, such processes may exist to maintain and regulate the intracellular spermidine level.

As mentioned previously, a rate comparison of putrescine export to putrescine uptake demonstrated an order of magnitude difference with similar *cis*-applied putrescine concentrations (Fig. 10A). This relatively greater rate of putrescine export appeared to contribute more significantly than putrescine uptake to maintaining the intracellular putrescine level measured in vivo and may lend support to reported low levels of intracellular putrescine in erythrocytes [54]. As described for spermidine, coordinated biosynthesis, protein binding or regulation of uptake and export processes may serve to maintain and regulate the intracellular level of putrescine [55–58].

Though the data for the non-saturable component of putrescine uptake supported a process mediated by simple diffusion, the non-saturable component of putrescine export appeared to be more complex. Since the permeability of the cell membrane for putrescine should be the same for inward or outward movement, putrescine uptake and export should exhibit equal rates if mediated by simple diffusion alone. The observed ten-fold greater permeability of putrescine export (Fig. 2 vs. Fig. 7), however, suggested that an additional export process may exist. This high-capacity putrescine export process may exhibit saturable kinetics if intracellular putrescine concentrations could be raised to higher levels and may be the same or different process as that determined for spermidine export.

Acknowledgements

We gratefully acknowledge the expertise and insights of Dr. Christian Lytle in the Division of Biomedical Sciences, University of California, Riverside, Riverside, CA. His valuable assistance and suggestions on the preparation of and kinetic characterization in human erythrocytes greatly aided these transport studies.

References

[1] Minchin, R.F., Raso, A., Martin, R.L. and Ilett, K.F. (1991) Eur. J. Biochem. 200, 457–462.
[2] Rinehart, C.A. and Chen, K.Y. (1984) J. Biol. Chem. 259, 4750–4756.
[3] Kobayashi, M., Iseki, K., Sugawara, M. and Miyazaki, K. (1993) Biochim. Biophys. Acta 1151, 161–167.
[4] Morgan, D.M.L. (1992) Biochem. J. 286, 413–417.
[5] Brachet, P. and Tomé, D. (1992) Biochem. Int. 27, 465–475.
[6] Sokol, P.P., Longnecker, K.L., Kachel, D.L. and Martin II, W.J. (1993) J. Pharm. Exp. Ther. 265, 60–66.
[7] Feige, J.J. and Chambaz, E.M. (1985) Biochim. Biophys. Acta 846, 93–100.
[8] De Smedt, H., Van der Bosch, L., Geuns, J. and Borghgraef, R. (1989) Biochim. Biophys. Acta 1012, 171–177.
[9] Bitonti, A.J., Dumont, J.A. and McCann, P.P. (1989) Biochem. Pharmacol. 38, 3638–3642.
[10] Davis, R.H. and Ristow, J.L. (1988) Arch. Biochem. Biophys. 267, 479–489.
[11] Davis, R.H. and Ristow, J.L. (1989) Arch. Biochem. Biophys. 271, 315–322.
[12] Heby, O. and Persson, L. (1990) Trends Biochem. Sci. 15, 153–158.
[13] Gonzalez, G.G. and Byus, C.V. (1991) Cancer Res. 51, 2932–2939.
[14] Jänne, J., Alhonen, L. and Leinonen, P.(1991) Ann. Med. 23, 241–259.
[15] Bueb, J.-L., Mousli, M. and Landry, Y. (1991) Agents Actions 33, 84–87.
[16] Pegg, A.E. (1988) Cancer Res. 48, 759–774.
[17] Byus, C.V. and Wu, V.S. (1991) J. Cell. Phys. 149, 9–17.
[18] Pegg, A.E. (1986) Biochem. J. 234, 249–262.
[19] Davis, R.H. (1990) J. Cell. Biochem. 44, 199–205.
[20] Pegg, A.E. and McGill, S. (1979) Biochim. Biophys. Acta 568, 416–427
[21] McCann, P.P., Pegg, A.E. and Sjoerdsma, A. (1987) Inhibition of Polyamine Metabolism: Biological Significance and Basis for New Therapies, Academic Press, Orlando, FL.
[22] Davis, R.H., Morris, D.R. and Coffino, P. (1992) Microbiol. Rev. 56, 280–290.
[23] Porter, C.W., Ganis, F., Libby, P.R. and Bergeron, R.J. (1991) Cancer Res. 51, 3715–3720.
[24] Kashiwagi, K., Miyamoto, S., Suzuki, F., Kobayashi, H., and Igarashi, K. (1992) Proc. Natl. Acad. Sci. USA 89, 4529–4533.
[25] Tjandrawinata, R.R., Hawel III, L. and Byus, C.V. (1994) J. Immunol. 152, 3039–3052.
[26] Hawel III, L., Tjandrawinata, R.R., Fukumoto, G.H. and Byus, C.V. (1994) J. Biol. Chem. 269, 7412–7418.

[27] Hawel III, L., Tjandrawinata, R.R. and Byus, C.V. (1994) Biochim. Biophys. Acta 1222, 15–26.
[28] Tjandrawinata, R.R. and Byus, C.V. (1995) Biochem. J. 305, 291–299.
[29] Tjandrawinata, R.R., Hawel, 3rd, L. and Byus, C.V. (1994) Biochem. Pharmacol. 48, 2237–2249.
[30] Hyvönen, T. (1989) Int. J. Biochem. 21, 313–316.
[31] Fulgosi, B., Colombatto, S. and Grillo, M.H. (1992) Int. J. Biochem. 24, 1461–1464.
[32] Mackarel, A.J. and Wallace, H.M. (1993) Biochem. Soc. Trans. 21, 50S.
[33] Wallace, H.M. (1990) Biochem. Soc. Trans. 18, 1079–1080.
[34] Coleman, C.S. and Wallace, H.M. (1990) Biochem. Soc. Trans. 18, 1228–1229.
[35] Saunders, N.A., Ilett, K.F. and Minchin, R.F. (1987) Biochim. Biophys. Acta 927, 170–176.
[36] Mitruka, B.M. (1981) Clinical Biochemical and Hematological Reference Values in Normal Experimental Animals and Normal Humans, Masson, New York.
[37] Belt, J.A., Marina, N.M., Phelps, D.A. and Crawford, C.A. (1993) Adv. Enzyme Reg. 33, 235–252.
[38] Cass, C.L., King, K.M., Montano, J.T. and Janowska-Wieczorek, A. (1992) Can. Res. 52, 5879–5886.
[39] Schroeder, C., Raynoschek, C., Fuhrmann, U., Damm, K., Venstrom, B. and Beug, H. (1990) Oncogene 5, 1445–1453.
[40] Moulinoux, J.-P., Le Calve, M. Quemener, V. and Quash, G. (1984) Biochimie 66, 385–393.
[41] Gilbert, R.S., Gonzalez, G.G., Hawel, L. and Byus, C.V. (1991) Anal. Biochem. 199, 86–92.
[42] Bauer, J.D. (1982) Clinical Laboratory Methods, The Mosby Co., St. Louis, MO.
[43] Fiocchi, O., Stabellini, G., Caruso, A., Masotti, M., Squerzanti, R., D'Orazi, D. and Farinelli, A. (1987) Int. J. Artif. Organs 10, 375–378.
[44] Purich, D.L. (1983) Contemporary Enzyme Kinetics and Mechanism: Selected Methods in Enzymology Series, Academic Press, Orlando, FL.
[45] Freifelder, D. (1982) Physical Biochemistry: Applications to Biochemistry and Molecular Biology, Freeman, New York.
[46] Brachet, P. Quemener, V., Havouis, R., Tome, D. and Moulinoux, J.P. (1994) Biochim. Biophys. Acta 1227, 161–170.
[47] Bogle, R.G., Mann, G.E., Pearson, J.D. and Morgan, D.M. (1994) Am. J. Physiol. 266, C776–783.
[48] Nadler, S.G. and Takahashi, M.T. (1985) Biochim. Biophys. Acta 812, 345–352.
[49] Houen, G. (1990) J. Chromatogr. 527, 146–151.
[50] Stein, W.D. (1986) Transport and Diffusion across Cell Membranes, Academic Press, Inc., Orlando, Florida.
[51] Nobel, P.S. (1983) Biophysical Plant Physiology and Ecology, Freeman, New York.
[52] Heinz, A. and Hoffman, J.F. (1990) Proc. Natl. Acad. Sci. 87, 1998– 2002.
[53] Scemama, J.L., Grabie, V. and Seidel, E.R. (1993) Am. J. Physiol. 265, G851–856.
[54] Gerbaut, L. (1991) Clin. Chem. 37, 2117–2120.
[55] Moulinoux, J.-P., Quemener, V. and Khan, N.A. (1991) Cell. Mol. Biol. 37, 773–783.
[56] Bratton, D.L. (1994) J. Biol. Chem. 269, 22517–22523.
[57] Moulinoux, J.P., Quemener, V., Havouis, R., Guille, F., Martin, C. and Seiler, N. (1991) AntiCancer Res. 11, 2143–2146.
[58] Sen, U. and Guha, S. (1990) Neoplasma 37, 521–526.